THE UNIVERSITY *of* EDINBURGH

Edinburgh Research Explorer

Diagnosis of river basins as CO2 sources or sinks subject to sediment movement

Citation for published version:
Yue, Y, Ni, J, Borthwick, AGL & Miao, C 2012, 'Diagnosis of river basins as CO2 sources or sinks subject to sediment movement' Earth Surface Processes and Landforms, vol 37, no. 13, pp. 1398-1406., 10.1002/esp.3254

Digital Object Identifier (DOI):
10.1002/esp.3254

Link:
Link to publication record in Edinburgh Research Explorer

Document Version:
Other version

Published In:
Earth Surface Processes and Landforms

Soil erosion and sediment transport induced CO_2 fluxes in river basins

Jinren Ni (Corresponding author)
The Key Laboratory of Water and Sediment Sciences, Ministry of Education, Beijing, P. R. China
Department of Environmental Engineering, Peking University, P. R. China
Address: No. 5 Yiheyuan Road, Haidian District, Beijing, China
Postal code: 100871
E-mail: nijinren@iee.pku.edu.cn
Tel.: +86-10-62751185
Fax.: +86-10-62756526

Yao Yue
The Key Laboratory of Water and Sediment Sciences, Ministry of Education, Beijing, P. R. China
Department of Environmental Engineering, Peking University, P. R. China

Alistair G. L. Borthwick
Dept of Civil and Environmental Engineering, University College Cork, Ireland

Chiyuan Miao
The Key Laboratory of Water and Sediment Sciences, Ministry of Education, Beijing, P. R. China
Department of Environmental Engineering, Peking University, P. R. China

Abstract: Soil erosion causes ecological deterioration of river basins. However, there is presently no consensus as to whether particular river basins act as erosion-induced CO_2 sources or sinks. This paper introduces a rule-of-thumb coordinate system based on sediment delivery ratio (*SDR*) and soil humin content (*SHC*) in order to identify the net effect of soil erosion and sediment transport on CO_2 flux in river basins. The *SDR*–*SHC* system delineates erosion-induced CO_2 source and sink areas, and further divides the sink into strong and weak areas according to the world-average line. In the *SDR*–*SHC* coordinate system, the Yellow River Basin, as a whole, appears to be a weak erosion-induced CO_2 sink (with an average annual CO_2 sequestration of ~ 0.235 Mt from 1960 to 2008, a relatively small value considering its 3.2% contribution to the World's soil erosion). The middle catchment overlapping the Loess Plateau is identified as the main source area, while the lower, the main sink. Temporal analysis shows that the Yellow River Basin was once an erosion-induced CO_2 source in the 1960s, but changed its role to become a weak erosion-induced CO_2 sink in the past 40 years due to both anthropogenic and climatic factors. The soil-related CO_2 fluxes are also examined for eight other major river basins in four continents. The basins considered in the Northern Hemisphere appear to be erosion-induced CO_2 sinks, while the two in the Southern Hemisphere act as erosion-induced CO_2 sources.

KEYWORDS: CO_2 flux; soil erosion; sediment transport

Introduction

Although it has long been acknowledged that soil erosion in river basins leads to ecological deterioration, the influence of soil erosion on the global carbon cycle has only recently been recognized. Regarded as a huge active carbon pool over the World's surface (Smith *et al*., 2001), soil exchanges carbon dioxide with the atmosphere through three mechanisms: chemical weathering of inorganic substances, organic carbon formation, and decomposition via biotic agents, all of which are affected greatly by soil erosion during the three processes of detachment, transport and deposition. Inorganic components like silicate or carbonate minerals in soil or rocks are weathered by runoff, consuming 0.26 to 0.30 Gt C annually (Berner *et al*., 1983; Meybeck, 1987; Amiotte Suchet *et al*., 1995). Compared to the inorganic processes, soil organic carbon (SOC) dynamics is more complicated. At an eroding site where soil detachment takes place, the newly exposed sub-layer containing less SOC has a tendency to absorb CO_2, because the original pedogenic equilibrium is broken when the SOC concentration is changed. Thus, the eroded carbon is partly replaced by new photosynthate. For Example, Clay *et al*. (2011) found that gully floors experience active photosynthesis during gully erosion. Recently, several researchers (Berhe *et al*., 2007; Quinton *et al*., 2010) have suggested a potential for stabilizing organic carbon at the freshly exposed mineral surface. While the detached soil is being delivered to low-lying places of a watershed, the soil aggregates break down, exposing previously encapsulated SOC to microbial attack (Lal *et al*., 2004) with an attendant increase in CO_2 emission. The eventual fate of the eroded soil diverges, with a fraction re-deposited within the catchment and the remainder ultimately washing into the sea. In the depositional part of a watershed, the original top-layer is protected from degrading by newly deposited sediment (Stallard, 1998). Meanwhile, the new top-layer decomposes at a higher rate because of the enrichment of soil carbon. Sediment in the anaerobic aquatic environment, on the other hand, remains well preserved (Cole *et al*., 2007). Anthropogenic factors also greatly affect carbon transfer processes. For example, vegetation restoration on bare land may benefit the carbon budget (by decreasing sources or increasing sinks, Worrall *et al*., 2011); conservation tillage characterized by enhanced C inputs and reduced erosion rates leads to a decrease of vertical C loss (Dlugoβ *et al*., 2011). A key point in understanding such complicated SOC dynamics is the interactive process between vegetation and erosion/deposition (Osterkamp *et al*., 2011).

Although there is universal agreement that the global chemical weathering of soil inorganic components is an important mechanism for CO_2 sequestration, the role of organic carbon loss remains controversial (Van Oost *et al*., 2004, 2008; Lal and Pimentel 2008; Kuhn *et al*., 2009). Several studies have concluded that the reduction of SOC in eroding soil represents a net source of erosion-induced CO_2 because of accelerated SOC mineralization. Polyakov and Lal (2008) carried out laboratory study of run-off induced soil erosion of a hillside, and found that up to 15% SOC was lost as CO_2 is released to the atmosphere. However, field observations suggest a much smaller decomposition proportion of SOC (Van Hemelryck *et al*., 2011). Assuming a mineralization fraction of 20 %, Lal (1995; 2003) estimated that globally 0.8–1.2 Gt C CO_2 is emitted every year. Taking a mass balance approach, Jacinthe and Lal (2001) calculated that about 0.37 Gt C CO_2 is released annually due to water erosion of cropland. Other studies have suggested a higher mineralization fraction from 50% to 100% (see e.g. Schlesinger, 1995; Óskarsson *et al*., 2004). Conversely, studies by Smith *et al*. (2001), McCarty and Ritchie (2002), Quine and Van Oost (2007), and Van Oost *et al*. (2007) have measured CO_2 sequestration due to erosion and deposition and inferred that hardly any decomposition of SOC takes place during sediment transport. Thus, the net flux is from the atmosphere to the ground. Smith *et al*. (2001) estimated that 1.0 Gt C CO_2 is sequestrated per year. McCarty and Ritchie (2002) devised a conceptual model which indicated that deposition in the wetland ecosystem might promote carbon sequestration at rate of 1.6–2.2 t C ha^{-1} yr^{-1}. Quine and Van Oost (2007) carried out field scale experiments and found that erosion induced a CO_2 sink of 9–14 g C m^{-2} yr^{-1}, the range of which was quite similar to previous model predictions by Liu *et al*. (2003). Van Oost *et al*. (2007) undertook further measurements at watershed scale, and extrapolated the findings to estimate the World's consumption of CO_2 to be ~0.12 Gt C.

Dymond (2010) estimated that the erosion-induced CO_2 sink in New Zealand could compensate for as much as 45 % of fossil emission. Hilton *et al*. (2011) also found that at a time scale of less than 100 yr, landslides in 13 rivers in New Zealand would lead to carbon sequestration.

There is an ongoing debate as to whether soil loss leads to an erosion-induced CO_2 source or sink, because different researchers have focused on certain aspects of the whole erosion process while ignoring others. The present paper aims to answer this question by considering both the stimulated pedogenic CO_2 sequestration in the newly-exposed carbon-poor top layer, and the accelerated CO_2 emission during sediment transport. Two parameters, the sediment delivery ratio (*SDR*) and the soil humin content (*SHC*), are used to indicate via a simple formula whether an erosion-induced CO_2 sink or source is likely to occur in a given river basin by calculating the vertical flux of CO_2 between the atmosphere and ground. A coordinate system based on *SDR* and *SHC* is used to visualize the net effect of soil erosion and sediment transport on CO_2 flux at basin scale. Particular attention is given to the Yellow River Basin, China, given that its middle reach passes through the Loess Plateau, one of the most severely eroding regions in the world. This model only considers continental processes. The flux generated by sediments exported into oceans has not been taken into account.

SDR–SHC system for assessing soil-induced CO_2 flux

Net CO_2 flux during the whole erosion process has three components: one from the eroding sites when topsoil is removed, a second induced by eroded soil that re-deposits, and a third related to the process of sediment transport. The net CO_2 flux budget is represented by

$$F_T = F_1 + F_2 + F_3, \quad (1)$$

where F is CO_2 flux (a positive value representing sequestration, a negative value indicating emission), and the subscripts T, 1, 2, and 3 refer to the total CO_2 flux, eroding soil CO_2 flux, re-deposited soil CO_2 flux, and sediment transport CO_2 flux. Van Oost *et al*. (2007) found a linear relationship between the vertical and lateral carbon fluxes at both erosion and deposition areas of a watershed,

$$F_1 = \alpha \cdot E_S \cdot C_{SOC}\ , \quad (2)$$

$$F_2 = \beta \cdot D_S \cdot C_{SOC}\ , \quad (3)$$

where α and β are the linear coefficients, E_S and D_S are the mass erosion and deposition of soil per annum respectively, and C_{SOC} is the ratio of SOC content to the total soil mass. Van Oost *et al*. did not measure the sediment transport flux. Although various researchers (Smith *et al*., 2001; Renwick *et al*., 2004; Van Oost *et al*. 2008) believed that the oxidation fraction of SOC during transport process is extremely low, Jacinthe *et al*. (2002) carried out field scale experiments which indicated that almost all the labile carbon contained in soil does degrade into CO_2 after erosion. Based on these experiments, Lal (2003) calculated the transport flux as the product of the mass loss of SOC ($E_S \cdot C_{SOC}$) and the decomposition proportion (P_D). However, the formula should be modified by replacing E_S with T_S (mass per annum of sediment transport), since Van Oost *et al.* (2007) has proved that sediments re-deposited within the basin hardly generate any fluxes,

$$F_3 = - T_S \cdot C_{SOC} \cdot P_D, \quad (4)$$

where the negative sign is used to indicate that the flux is from ground to atmosphere. Although there is disagreement in the published literature as to how much SOC contained in the exported sediment will be oxidized (see e.g. Schlesinger, 1995; Lal, 2003; Óskarsson *et al*., 2004), the core ideas are similar: namely, that labile soil carbon decomposes into CO_2 whereas recalcitrant carbon remains stable. Raymond and Bauer (2001) analyzed radiocarbon data obtained at the estuaries of four rivers at different scales, and discovered that most of the young organic carbon in riverine sediments was selectively degraded, while the old and refractory components were exported into the ocean. Jacinthe *et al*. (2002) examined runoff sediments and found that 100 % of the labile organic carbon was decomposed within an observation period of 100 days, and about 50 % was degraded within 20 days. Óskarsson *et al*. (2004) summarized the oxidation fraction of sediments from different rivers discharging into the Gulf of Lions, the Gulf of Mexico, the Arctic Ocean, and the North Atlantic during sediment transport, and concluded that the decomposition proportion depends on the decomposability of organic carbon. Óskarsson *et al*. also classified soil organic matter (SOM) into the following five categories: carbohydrates, lipids, lignin-derived substances, humic acid and humin. Of these, humin is usually recalcitrant and decomposes very slowly. Thus, Óskarsson *et al*. suggested that , in Iceland, the active components were oxidized, whereas the passive component persisted. Based on the same assumption, we make the approximation that

$$P_D = 1 - SHC, \tag{5}$$

where *SHC* stands for the Soil Humin Content in the SOC, since the actual decomposition proportion is hard to estimate. Then, we obtain the deposition potential, i.e. the maximum risk of CO_2 emission. *SHC* is calculated as the ratio of humic carbon content to the total organic carbon mass, a dimensionless parameter varying from 0 to 1. Combining Equations 1 ~ 5, the net CO_2 flux in the entire erosion process is written:

$$F_T = \alpha \cdot E_S \cdot C_{SOC} + \beta \cdot D_S \cdot C_{SOC} - T_S \cdot C_{SOC} \cdot (1 - SHC), \tag{6}$$

We define the sediment delivery ratio (*SDR*) as the ratio of transported mass to eroded soil mass; in other words,

$$SDR = T_S / E_S. \tag{7}$$

Noting that,

$$D_s = E_s - T_s, \tag{8}$$

Equation (6) can then be written as

$$F_T = \alpha \cdot E_S \cdot C_{SOC} + \beta \cdot \mathrm{E}_S \cdot C_{SOC}(1 - \mathrm{SDR}) - E_S \cdot C_{SOC} \cdot \mathrm{SDR} \cdot (1 - SHC). \tag{9}$$

Defining the vertical flux ratio *VFR* as the ratio of vertical carbon flux to the lateral carbon flux, we have

$$F_T = E_S \cdot C_{SOC} \cdot VFR. \tag{10}$$

Hence, by comparing Equation (9) with Equation (10),

$$VFR = (\alpha + \beta) - SDR\,(1 - SHC + \beta). \tag{11}$$

Equation (11) indicates whether a basin acts as an erosion-induced CO_2 source or sink. For *VFR* > 0, soil erosion results in an erosion-induced CO_2 sink; whereas for *VFR* < 0, the basin is a CO_2 source. A critical condition occurs when *VFR* = 0, and the basin neither emits nor absorbs CO_2. For a given value of lateral carbon flux, the larger the magnitude of *VFR* the greater the strength of the erosion-induced CO_2 sink or source (depending on the sign of *VFR*). So, *VFR* is a single parameter that characterizes the strength of the CO_2 flux, and whether it is an erosion-induced CO_2 source or sink. Van Oost *et al.* (2007) parameterized α and β to be 0.26 and 0 respectively and further used the two values to calculate the world's total erosion-induced CO_2 flux. As the sampled soil profiles covered a wide variety of climatic and pedogenic conditions, Van Oost *et al.*'s estimates of α and β can approximate the World's average level, if no better estimates are available. Thus,

$$VFR = 0.26 - SDR\,(1 - SHC), \tag{12}$$

for the World's average condition. Figure 1 plots the critical line for *VFR* = 0 on the *SDR*-*SHC* coordinate system, which divides the 1×1 square containing all possible combinations of *SDR* and *SHC* into two parts. The region above and to the left of the critical line represents all the erosion-induced CO_2 sink areas, while the remainder represents the erosion-induced CO_2 source areas. Using this approach, we can immediately determine whether any given basin is an erosion-induced CO_2 sink or source provided *SDR* and *SHC* are known.

The world average level of *VFR* = 0.21 (supposing *SDR* = 0.1 and *SHC* = 0.5; Lal, 2003; Óskarsson *et al*., 2004) indicates that the World's river basins act together as a carbon sink. In Figure 1, the World-average value of *VFR* is used to provide another demarcation line, whereby the erosion-induced CO_2 sink region of the *SDR*–*SHC* system is further divided into two parts. The sub-region above and to the left of this demarcation line represents basins with above World-average CO_2 sequestration potentials (i.e. strong erosion-induced CO_2 sink), whereas the central sub-region represents basins with lower sequestration potentials (i.e. weak erosion-induced CO_2 sink).

CO_2 flux in the Yellow River Basin

The Yellow River Basin is one of the major contributors to the World's river sediment exchange. Its catchment area is huge, and contains regions that are suffering intense soil erosion. In this section, we investigate whether the enormous sediment yield of the Yellow River Basin (3.2 % of the World's total) contributes an equally significant CO_2 flux to the total World flux induced by soil erosion, and whether the Yellow River Basin affects the climatic system through emitting/absorbing CO_2 to the same extent as it does the ecological environment.

Study Area

The Yellow River flows through seven provinces and two autonomous regions of northern China, and is of length 5464 km. Its annual discharge at the river mouth, averaged over the period from 1960 to 2008, is about 52 × 10^9 m^3, 63 % of which is from the upper reaches. The Yellow River Basin (Figure 2) extends from 96 to 119 ^{o} E longitude and from 32 to 42 ^{o} N in latitude, has an area of 0.752 million km^2, and supports a population of 107 million. It has a continental monsoon climate, with annual precipitation ranging from 300 mm in the northwest to 700 mm in the southeast (Ni *et al.*, 2008). The middle reach of the Yellow River passes through the Loess Plateau which is experiencing major environmental degradation through advanced soil erosion. In the 1970s, the mean annual yield of sediment of the Yellow River Basin was 1.40 × 10^9 tons. Soil conservation measures implemented by the Yellow River Conservancy Commission reduced the mean sediment discharge in the period from 2000 to 2008 to about 0.36 × 10^9 tons. In spite of this, there remains a considerable risk of the sediment discharge rising to its former high values should the runoff increase.

Data Presentation

Data on sediment yield, soil distribution and composition were utilized in estimating the CO_2 flux of the Yellow River Basin. Sediment discharge data from 1960 to 2008 at Sanmenxia and Lijin (Figure 3) provided by the Yellow River Conservancy Commission (YRCC) were used to quantify the soil erosion and sediment yield. The sediment discharge data series display a significant decreasing trend, due to the successful implementation of soil conservation projects over the past 30 years. A 1:1000000 map (Figure 2) of soil distribution in the Yellow River Basin has been digitalized and the area of each type obtained using ArcGIS. Soil composition data were supplied by the Soil Survey Office of China, and the key properties are listed in Table 1. The content of SOC and humin, as a function of soil type, local environment and depth, vary widely across the Yellow River Basin. There are 24 types of soils in the basin, of C_{SOC} ranging from 2.24×10^{-3} to 29.50×10^{-3}. The more fertile soil is primarily distributed in the southwest of the basin, whereas infertile soil is found in the central and eastern areas.

SDR, *SHC* and SOC content of the Yellow River Basin

The sediment delivery ratio (*SDR*) is the ratio of sediment yield to the total erosion. *SDR* is affected by many factors such as the geological and morphological conditions, scale, runoff, river configuration, soil structure, vegetation and land use of the basin (Walling, 1983; Ebisemiju, 1990). Previous studies of *SDR* in the Yellow River Basin have focused on the middle reach where more than 90% of the total sediment in the river is supplied from the eroding Loess Plateau. In this region, the sediment comprises fine silt with particle diameters mostly < 0.05 mm, the stream-wise bed slope of the middle reach is steep, *SDR* ~ 1 (Xu, 1999), and sediment yield almost equals sediment erosion. Thus, the sediment discharge at the downstream end of the middle reach at Sanmenxia can be taken as an approximate measure of the total amount of erosion in the whole basin. Given the measurements of estuarine sediment discharge at Lijin, the *SDR* of the Yellow River Basin is determined as the ratio of sediment yields at Lijin to Sanmenxia. In the period from 1960 to 2008, the average sediment discharges at Sanmenxia and Lijin are 0.641 and 0.926 Gt, and so the average *SDR* of the Yellow River Basin is 0.692. Table 1 summarizes *SHC* and C_{SOC} according to soil type in the Yellow River basin, from which the area-weighted average *SHC* and C_{SOC} of the Yellow River Basin are 6.15×10^{-3} and 0.684.

Magnitude of CO_2 flux

Given the known values of C_{SOC}, *SHC*, *SDR* and *T*s, the average erosion-induced CO_2 flux from 1960 to 2008 in the Yellow River Basin is calculated to be a net erosion-induced CO_2 sink of strength 0.235 $Mt.yr^{-1}$ using Equation (10) and Equation (12). By also assuming that the total sediment discharge in the world is 20 Gt per year (Smith *et al*., 2001), the SOC content is 2%, the *SDR* is 0.1 (Lal, 2003), and the *VFR* is 0.21, Equation (10) gives the World's total CO_2 flux to be a net erosion-induced CO_2 sink of 0.84 Gt C per year. This confirms our previous observation that most river basins in the World act as erosion-induced CO_2 sinks. However, the magnitude of CO_2 flux absorbed by the Yellow River Basin is very small considering its great contribution to World sediment yield. Table 3 provides a quantitative comparison between the values of CO_2 flux, sediment delivery ratio, etc. for the World and the Yellow River Basin. The small magnitude of CO_2 sequestration by the Yellow River Basin is related to its small value of *VFR* and the loess SOC content, as well as a *SDR* significantly above the World-average level.

Since *SHC* mainly depends on climate, and *SDR* is related to the area of the drainage basin, spatial analysis of CO_2 flux is necessary to answer the question as to whether there is a progressive shift from source to sink from the river source to mouth. With this in mind, five hydrometric stations at Hekou, Longmen, Sanmenxia, Huayuankou, and Lijin, are selected at different locations along the main channel. Hekou is located close to the interface between the upper and middle reaches of the Yellow River, Sanmenxia is close to the interface between the middle and lower reaches, and Lijin is the mouth of the river. To calculate the CO_2 flux of the upper and middle reaches, Equations 7, 10, and 12 are combined to give:

$$F_T = T_S\, C_{SOC}[0.26 - SDR\,(1\text{-}SHC)]/SDR, \quad (13)$$

where T_S can be estimated as the difference between sediment transport at two adjacent stations. Average *SHC* and C_{SOC} can be derived from DEM data and soil distribution map, using the ArcGIS hydrology and intersect tools. Generally, *SDR* tends to decrease downstream as the slope gets less steep in the lower part where deposition occurs. Nevertheless, this is not the case for the Yellow River which passes through the Loess Plateau and generates a very high *SDR* (~1, Xu, 1999) in the middle catchment. In the upper region of the basin, however, *SDR* is about 0.95 (Li and Liu, 2006). Since the bed elevation of the lower reach is higher than the adjacent ground beyond the river banks due to sediment deposition on the riverbed between dykes, no lateral flow enters. Therefore, this region is the main depositional area of the basin. Though having experienced mineralization during delivery process before settling, the depositional sediments neither absorb nor emit CO_2 in the long run (Dymond, 2010). This fact implies that the decomposed SOC can be recovered after deposition. So, the CO_2 flux into the lower catchments is as much as the previous SOC decomposition during sediment transport:

$$F_T = D_S\, C_{SOC}\, (1 - SHC), \qquad (14)$$

where D_S can be calculated from the difference of sediment transport rates at two adjacent stations. Figure 4 plots the accumulative CO_2 flux from river source to mouth using Equations 13 and 14. The plot shows that the upper region of the Yellow River Basin acts as a faint source of 0.03 Mt/yr, the middle catchment is the main source (0.18 Mt/yr) of the basin, and the depositional region brings about a 0.42 Mt/yr sink. Such results imply that application of soil conservation measures (such as sediment check dams) to the Loess Plateau might have the additional benefit of reducing CO_2 emission in the basin.

Supposing that the average *SHC* of the Yellow River Basin remains constant, the decadal changes of *VFR* and *SDR* can be derived from recorded sediment discharge data (provided by YRCC) covering a period from 1960 to 2008 (Figure 5). The results imply that although the Yellow River Basin has acted as a net erosion-induced CO_2 sink over the past 49 years, it was once a CO_2 emitter during the 1960s, and has been altered to become an erosion-induced CO_2 sink since the 1970s. Despite the erosion-induced CO_2 sink apparently weakening slightly in the 1980s, it strengthened in the 1990s and 2000s. The increase/decrease of *VFR* is primarily due to the decrease/increase of *SDR*. In the 1970s, the construction of large reservoirs, such as those at Liujiaxia, Guxian, Qingtongxia, and Longyangxia, significantly reduced the *SDR* of the Yellow River Basin. Since the 1990s, with the climate in the Yellow River Basin becoming drier, the discharge at the estuary has sharply decreased (Miao *et al.*, 2011). Consequently, the capability of sediment transport has become smaller.

Global Role of Yellow River Basin

The (*SDR*, *SHC*) coordinates of the Yellow River Basin, the Yangtze Basin, the Ganges Basin in Asia, the Congo Basin, the Niger Basin, the

Orange Basin, the Senegal Basin in Africa, the Mississippi Basin in North America, and the Rhine Basin in Europe are plotted in Figure 1, along with solid lines that demark the erosion-induced CO_2 source, weak sink, and strong sink regions. Since the soil survey data is lack in river basins other than the Yellow River Basin, the ratio of POC (Particulate Organic Carbon) flux to the total SOC flux is used to approximate to *SHC*. Considering the fact that only a small proportion of the un-decomposed SOC other than humin exists in the POC discharge (10% ~ 20%, Chen, 2006), such approximation may lead to a slight over-estimation of *SHC*. However, considering that the replacement of the decomposition proportion (P_D) with the non-humin content in the SOC (i.e. 1–*SHC*) in Equation 4 introduced an over-estimation of CO_2 emission by giving the maximum emission risk, deviation from *SHC* might close the gap between the emission potential and the real flux to some extent. The raw data are listed in Table 2. Here, we take $F_{POC}/C_{SOC}Fs$ (the ratio of Particulate Organic Carbon flux to the total SOC content defined as flux) to be an approximation to *SHC*. It is interesting to see that the Congo Basin and the Orange Basin in the Southern Hemisphere are erosion-induced CO_2 sources, while the Yellow River Basin, the Yangtze Basin, the Ganges Basin, the Niger Basin, the Senegal Basin, the Mississippi Basin, and the Rhine Basin in the Northern Hemisphere are erosion-induced CO_2 sinks. Among the nine basins, the Senegal Basin in the West Africa is the sole basin to be a strong sink of erosion-induced CO_2 flux.

The uncertainties on the estimation of soil erosion, sediment delivery, soil properties, and the two linear coefficients, α and β, were quantified using a Monte Carlo analysis. *SDR*, *SHC*, α, and β were varied randomly using a normal distribution. The standard deviations of α and β were calculated according to Van Oost *et al.*'s experimental data. For *SDR* and *SHC*, it was assumed that the standard deviation $\sigma = \mu/4$ where μ is the expected value. 1000 independent simulations were carried out for every one of the nine basins. The world average level of *VFR* was re-calculated every time for each pair of α and β. The simulation results listed in Table 4 show that the confidence probabilities of the discrimination for erosion-induced CO_2 sinks or sources are all above 53.5%. The probability levels are even above 75% in the Yangtze Basin, the Congo Basin, the Niger Basin, the Orange Basin, the Senegal Basin, and the Mississippi Basin.

Discussion

Error Analysis

Computation of *SHC* of the Yellow River Basin as an area-based weighted average introduces error, given that *SHC* is plotted against *SDR* of the entire catchment. The contribution of sediment from each soil type listed in Table 1 is not proportional to their area. In other words, most of the sediment probably originates from land under cultivation or grazing while sediment originated from other types of soil might not be present at all. However, as the contribution of each soil type to sediment yield is hard to estimate, the area-weighted-averaging method provides a means of approximating the average *SHC* based on sediment yield. In this section, the error introduced by such approximation is analyzed.

The average *SHC* based either on sediment yield or on distribution area is estimated from:

$$\overline{SHC} = \frac{\sum Y_i SHC_i}{\sum Y_i} \tag{15}$$

and

$$\overline{SHC}' = \frac{\sum A_i SHC_i}{\sum A_i}, \tag{16}$$

where Y_i, A_i, and SHC_i represent sediment yield, area, and SHC, respectively, in the *i*-th basin unit (with uniform sediment yield intensity and soil distribution). The sediment yield is the product of sediment yield modulus and area:

$$Y_i = M_i A_i . \tag{17}$$

By substituting Equation 17 into Equations 15 and 16, the relative error of $\overline{SHC}'$ compared to $\overline{SHC}$ is:

$$Error = \frac{|\overline{SHC}' - \overline{SHC}|}{\overline{SHC}}$$

$$= \frac{|\sum Y_i / \sum A_i \cdot \sum A_i SHC_i - \sum M_i A_i SHC_i|}{\sum M_i A_i SHC_i}. \tag{18}$$

Let:

$$\sum Y_i / \sum A_i = \overline{M}, \tag{19}$$

where $\overline{M}$ is the average sediment yield modulus of the basin. Thus,

$$Error = \frac{\sum A_i SHC_i |\overline{M} - M_i|}{\sum A_i SHC_i M_i}. \quad (20)$$

Suppose that:

$$|\overline{M} - M_i| \le 2\sigma \overline{M}, \quad (21)$$

where σ is the standard deviation. So,

$$|1-2\sigma|\overline{M} \le M_i \le |1+2\sigma|\overline{M}. \quad (22)$$

Combining Equations 20, 21 and 22, we have:

$$Error \le \frac{2\sigma}{|1-2\sigma|}. \quad (23)$$

That is to say, the replacement of sediment-yield-based average *SHC* with the area-weighted average leads to a maximum relative error of $\frac{2\sigma}{|1-2\sigma|}$.

Comparison with High Standing Islands

High standing islands (like Taiwan, Indonesia, Malaysia, etc.) comprise only 3 % of the world's land mass, but contribute to 17 % ~ 35 % of the total POC flux (Lyons *et al.*, 2002). This implies that carbon cycling may be very active at high standing islands, and the erosion process in such areas can exert important influence on the CO_2 flux between the soil and the atmosphere. For example, New Zealand (which can be viewed as representative of high standing islands) is characterized by high precipitation, severe erosion, and consequently, considerable sediment transport. To calculate the erosion-induced CO_2 flux in New Zealand, Dymond (2010) has considered soil regeneration at erosion sites, CO_2 release during sediment delivery, and carbon transfer related to soil deposition, which are also the three key processes described in the *SDR-SHC* model. The results show that New Zealand acts as net erosion-induced CO_2 sink, with annual carbon absorption of 3.1 (-2.0/+2.5) Mt. Given that the SOC erosion over the country is 4.8 Mt/yr, the *VFR* of New Zealand is 0.65 (Equation 9), far above the World-average level of 0.21. By comparison, the *VFR*s of the nine large continental rivers in Table 2 are well below the World-average level. Even the Senegal River which acts as the single "Strong Erosion-induced Sink" of the nine rivers has a CO_2 sequestration capacity (*VFR*) only one-third that of New Zealand. The relatively larger CO_2 sequestration capacity probably results from the higher marine burial efficiency of SOC on high standing islands, which brings about a smaller SOC decomposition coefficient compared to large river systems (Masiello, 2007; Dymond, 2010). On the other hand, the biological productivity in New Zealand is also large, which means a higher soil regeneration rate (Dymond, 2010).

Conclusions

In the Abstract, we noted that there is disagreement between experts on the role of river basins in carbon exchanges with the atmosphere during soil weathering, erosion, and transport. The present paper has proposed a conceptually simple method for assessing carbon flux emissions from, and capture by river basins. It should be noted that the method is essentially rule-of-thumb, and makes several rather sweeping assumptions about the processes related to erosion-induced SOC balance. Nevertheless, we believe the approach is useful as a guide to carbon flux exchanges in river basins, provided the results are treated critically. The paper develops an identification system based on sediment delivery ratio (*SDR*) and soil humin content (*SHC*), which indicates whether a given region is either an erosion-induced carbon source or sink, and its relative strength. A single parameter, the vertical flux ratio, $VFR = 0.26 - SDR\ (1 - SHC)$ can be used to demark the carbon flux characteristics of single or multiple river basin(s). The Yellow River Basin, as a whole, has acted as a weak erosion-induced CO_2 sink on average over the past 49 years. The middle catchment overlapping the Loess Plateau appears to be the main source area, whereas the lower reach is the main sink. Temporal analysis indicates that the Yellow River Basin was once an erosion-induced CO_2 source. However, the combination of human activities related to the construction of large reservoirs and climate change caused CO_2 emission to decrease in the 1960s, after which the Yellow River Basin changed role to become a weak erosion-induced CO_2 sink. Analysis of published data using the *SDR*–*SHC* system has shown that of nine major river basins considered, all appear to be erosion-induced CO_2 sinks except the Congo Basin and the Orange Basin in the Southern Hemisphere. Compared to large river basins, the high standing islands comprising a very small proportion of the World's land mass seem to have considerable capacity of CO_2 sequestration. The present study represents a step towards resolving the controversy on whether erodible river basins are either erosion-induced CO_2 sinks or sources. Yet, the lack of data on soil properties as well as erosion and sediment transport of large-scale basins introduce uncertainties into the present research. For example, the approximation to average *SHC* of the Yellow River Basin based on an area-weighted method would introduce a maximum relative error of $\frac{2\sigma}{|1-2\sigma|}$, where σ is the standard deviation of sediment yield modulus. Moreover, the assumption that deposited sediments act as neither a significant sink nor source (Van Oost *et al.*, 2007) still needs more substantive evidence, given that there is no consensus as to whether SOC deposited on land is sequestered or not.

Acknowledgements – Financial support from the National Basic Research Program of China (2007CB407202) is gratefully acknowledged.

References

Asselman NEM, Middelkoop H, van Dijk PM. 2003. The impact of changes in climate and land use on soil erosion transport and deposition of suspended sediment in the River Rhine. *Hydrological Processes* **17:** 3225–3244. doi: 10.1002/hyp.1384.

Amiotte Suchet P, Probst JL. 1995. A global model for present-day atmospheric/soil CO2 consumption by chemical erosion of continental rocks (GEM–CO2). *Tellus* **47B:** 273–280. doi: 10.1034/j.1600-0889.47.issue1.23.x.

Berhe AA, Harte J, Harden JW, Torn MS. 2007. The significance of the erosion-induced terrestrial carbon sink. *Bioscience* **57:** 337–346. doi: 10.1641/B570408.

Berner RA, Lasaga AC, Garrels RM. 1983. The carbonate–silicate geochemical cycle and its effect on atmospheric carbon dioxide over the past 100 million years. *American Journal of Science* **283:** 641–683. doi: 10.2475/ajs.283.7.641.

Chen JS. 2006. *Fundamentals of River Water Quality and Chinese River Water Quality*. Science Press: Beijing.

Clay GD, Dixon S, Evans MG, Rowson JG, Worrall F. 2011. Carbon dioxide fluxes and DOC concentrations of eroding blanket peat gullies. *Earth Surface Processes and Landforms*. doi: 10.1002/esp.3193

Cole JJ, Prairie YT, Caraco NF, McDowell WH, Tranvik LJ, Striegl RG, Duarte CM, Kortelainen P, Downing JA, Middelburg JJ, Melack J. 2007. Plumbing the global carbon cycle: Integrating inland waters into the terrestrial carbon budget. *Ecosystems* **10:** 171–184. doi: 10.1007/s10021-006-9013-8.

Dlugoß V, Fiener P, Van Oost K, Schneider K. 2011. Model based analysis of lateral and vertical soil carbon fluxes induced by soil redistribution processes in a small agricultural catchment. *Earth Surface Processes and Landforms*. doi: 10.1002/esp.2246

Dymond JR. 2010. Soil erosion in New Zealand is a net sink of CO2. *Earth Surface Processes and Landforms* **35**(15): 1763–1772, doi: 10.1002/esp.2014

Ebisemiju FS. 1990. Sediment delivery ratio prediction equations for short catchment slopes in a humid tropical environment. *Journal of Hydrology* **114:** 191–208. doi: 10.1016/0022-1694(90)90081-8.

Hilton RG, Meunier P, Hovius N, Bellingham PJ, Galy A. 2011. Landslide impact on organic carbon cycling in a temperate montane forest. *Earth Surface Processes and Landforms* 36(12): 1670–1679, doi: 10.1002/esp.2191

Jacinthe PA, Lal R. 2001. A mass balance approach to assess carbon dioxide evolution during erosional events. *Land Degradation Development* **12:** 329–339. doi: 10.1002/ldr.454.

Jacinthe PA, Lal R. Kimble JM. 2002. Carbon dioxide evolution in runoff from simulated rainfall on long-term no-till and plowed soils in southwestern Ohio. *Soil and Tillage Research* **66:** 23–33. doi: 10.1016/S0167-1987(02)00010-7.

Kuhn NJ, Hoffmann T, Schwanghart W, Dotterweich M. 2009. Agricultural soil erosion and global carbon cycle: controversy over? *Earth Surface Processes and Landforms* **34:** 1033–1038. doi: 10.1002/esp.1796.

Lal R. 1995. Global soil erosion by water and carbon dynamics in *Soils and Global Change,* Lal R et al. (eds): 131–142. CRC/Lewis Publishers: Boca Raton Florida.

Lal R. 2003. Soil erosion and the global carbon budget. *Environment International* **29:** 437–450. doi: 10.1016/S0160-4120(02)00192-7.

Lal R, Griffin M, Apt J, Lave L, Morgan G. 2004. Response to comments on "Managing soil carbon". *Science* **305:** 1567d. doi: 10.1126/science.1101271.

Lal R, Pimentel D. 2008. Soil Erosion: A carbon sink or source? *Science* **319:** 1040–1042. doi: 10.1126/science.319.5866.1040.

Li ZG, Liu BZ. 2006. Calculation on soil erosion amount of main river basins in China. *Science of Soil and Water Conservation 4:* 1–6 (in Chinese). doi: cnki: ISSN: 1672-3007.0.2006-02-000.

Liu S, Bliss N, Sundquist E, Huntington TG. 2003. Modeling carbon dynamics in vegetation and soil under the impact of soil erosion and deposition. *Global Biogeochemical Cycles* **17:** 1074–1097. doi: 10.1029/2002GB002010.

Ludwig W, Probst JL, Kempe S. 1996. Predicting the oceanic input of organic carbon by continental erosion. *Global Biogeochemical Cycles* **10:** 23–41. doi: 10.1029/95GB02925.

Lyons WB, Nezat CA, Carey AE, Hicks DM. 2002. Organic carbon fluxes to the ocean from high-standing islands. *Geology* **30**: 443–446.

Masiello CA. 2007. Quick burial at sea. *Nature* **450**: 360–361.

McCarty GW, Ritchie JC. 2002. Impact of soil movement on carbon sequestration in agricultural ecosystems. *Environmental Pollution* **116:** 423–430. doi: 10.1016/S0269-7491(01)00219-6.

Meybeck M. 1982. Carbon nitrogen and phosphorus transport by world rivers. *American Journal of Science* **282:** 401–450. doi: 10.2475/ajs.282.4.401.

Miao CY, Ni JR, Borthwick AGL, Yang L. 2011. A preliminary estimate of human and natural contributions to the changes in water discharge and sediment load in the Yellow River. *Global and Planetary Change* **76:** 196–205. doi: 10.1016/j.gloplacha.2011.01.008.

Ni JR, Li XX, Borthwick AGL. 2008. Soil erosion assessment based on minimum polygons in the Yellow River basin China. Geomorphology **93:** 233–252. doi: 10.1016/j.geomorph.2007.02.015.

Óskarsson H, Arnalds Ó, Gudmundsson J, Gudbergsson G. 2004. Organic carbon in Icelandic Andosols: geographical variation and impact of erosion.

Catena **56:** 225–238. doi: 10.1016/j.catena.2003.10.013.

Osterkamp WR, Hupp CR, Stoffel M. 2011. The interactions between vegetation and erosion: new directions for research at the interface of ecology and geomorphology. *Earth Surface Processes and Landforms*, doi: 10.1002/esp.2173

Polyakov VO, Lal R. 2008. Soil organic matter and CO_2 emission as affected by water erosion on field runoff plots. *Goederma.* **143:** 216–222. doi: 10.1016/j.geoderma.2007.11.005.

Quine TA, Van Oost K. 2007. Quantifying carbon sequestration as a result of soil erosion and deposition: retrospective assessment using caesium-137 and carbon inventories. *Global Change Biology* **13:** 2610–2625. doi: 10.1111/j.1365-2486.2007.01457.x.

Quinton JN, Govers G, Van Oost K, Dardgett RD. 2010. The impact of agricultural soil erosion on biogeochemical cycling. *Nature Geoscience* **3:** 311–314. doi:10.1038/ngeo838.

Raymond, P.A., Bauer, J.E., 2001. Riverine export of aged terrestrial organic matter to the North Atlantic Ocean. *Nature* **409**, 497– 500

Renwick WH, Smith SV, Sleezer RO, Buddemeier R. W. 2004. Comment on ‘‘Managing soil carbon’’ (II). *Science* **305:** 1567c. doi: 10.1126/science.1100447.

Schlesinger WH. (1995) Soil respiration and changes in soil carbon stocks in *Biotic feedbacks in the global climatic system: will the warming feed the warming?* Woodwell GM, Mackenzie FT (eds): 159–168. Oxford University Press: New York.

Smith SV, Renwick WH, Buddenmeier RW, Crossland CJ. 2001. Budgets of soil erosion and deposition for sediments and sedimentary organic carbon across the conterminous United States. *Global Biogeochemical Cycles* **15:** 697–707. doi: 10.1029/2000GB001341.

Smith SV, Sleezer RO, Renwick WH, Buddemeier RW. 2005. Fates of eroded soil organic carbon: Mississippi Basin case study. *Ecological Applications* **15:** 1929–1940. doi: 10.1890/05-0073.

Stallard RF. 1998. Terrestrial sedimentation and the carbon cycle: coupling weathering and erosion to carbon burial. *Global Biogeochemical Cycles* **12:** 231–257. doi: 10.1029/98GB00741.

Van Hemelryck H, Govers G, Van Oost K, Merckx R (2011) Evaluating the impact of soil redistribution on the in situ mineralization of soil organic carbon. *Earth Surface Processes and Landforms* **36**(4): 427–438,

Van Oost K, Govers G, Quine TA. Heckrath G. 2004. Comment on ‘‘Managing soil carbon’’ (I). *Science* **305:** 1567b. doi: 10.1126/science.1100273.

Van Oost K, Quine TA, Govers G, De Gryze S, Six J, Harden JW, Ritchie JC, McCarty GW, Heckrath G, Kosmas C, Giraldez JV, Marques da Silva JR, Merckx R. 2007. The impact of agricultural soil erosion on the global carbon cycle. *Science* **318:** 626–629. doi: 10.1126/science.1145724.

Van Oost K, Six J, Govers G, et al. 2008. Soil erosion: A carbon sink or source? Response. *Science* **319:** 1042–1042.

Walling DE. 1983. The sediment delivery problems. Journal of Hydrology **65:** 209–237. doi: 10.1016/0022-1694(83)90217-2.

Worrall F, Rowson JG, Evans MG, Pawson R, Daniels S, Bonn A. 2011. Carbon fluxes from eroding peatlands – the carbon benefit of revegetation following wildfire. *Earth Surface Processes and Landforms* **36**(11): 1487–1498, doi: 10.1002/esp.2174

Xu JX. 1999. Erosion caused by hyperconcentrated flow on the Loess Plateau of China. *Catena* **36:** 1–19.

Zhang X, Drake N, Wainwright J. 1998. Downscaling land surface patameters for global soil erosion estimation using no ancillary data. *Proceedings of the 3rd International Conference on Geo-Computation*, University of Bristol, UK.

Table 1. Soil properties in the Yellow River Basin *

Soil Type	Distribution Area (10^3 km^2)	C_{SOC} (g·kg^{-1})	*SHC*
aeolian soils	66	3.93	0.565
black loess soils	19	6.75	0.404
black soils	2	26.15	0.623
brown caliche soils	29	n.a.**	n.a.
brown earths	19	2.31	0.628
castano-cinnamon soils	19	n.a.	n.a.
castanozems	42	8.60	0.628
chernozems	8	29.50	0.713
cinnamon soils	76	6.88	0.619
cold calcic soils	1	9.76	0.766
dark felty soils	44	n.a.	n.a.
felty soils	70	n.a.	n.a.
fluvo-aquic soils	41	n.a.	n.a.
frigid calcic soils	17	19.72	0.749
frigid frozen soils	5	7.80	0.769
gray desert soils	2	2.96	0.769
gray-cinnamon soils	23	n.a.	n.a.
irrigation silting soils	10	7.00	0.757
loessial soils	166	2.24	0.789
neo-alluvial soils	28	n.a.	n.a.
sierozems	34	13.60	0.772
skeletal soils	23	n.a.	n.a.
solonchaks	8	3.31	0.547
Average		6.15	0.684

*: C_{SOC} and SHC data of each soil type are obtained from analytical experiments on typical soil profiles sampled by the Soil Survey Office of China. Soil distribution areas are extracted from 1:1000000 digital map supplied by the Institute of Soil Science, Chinese Academy of Sciences.

**: n.a. stands for not available.

Table 2. Data for nine river basins

Continent	No.	Name	Area[a] 10^6 km^{-2}	Fs[a] t·km^{-2}·yr^{-1}	E[b] mm·yr^{-1}	*SDR*	$F_{POC}/C_{SOC}Fs$	*VFR*
Asia	1	Yangtze	1.817	250		0.174[d]	0.473	0.168
	2	Ganges	1.648	668	1.179	0.378	0.403	0.034
Africa	3	Congo	3.704	11	0.016	0.458	0.086	-0.159
	4	Niger	1.54	33	0.133	0.165	0.354	0.153
	5	Orange	0.716	100	0.143	0.466	0.154	-0.134
	6	Senegal	0.369	8	0.133	0.040	0.095	0.224
America	7	Mississippi	3.243	120		0.203[e]	0.216	0.101
Europe	8	Rhine	0.156	11.7		0.150[f]	0.599	0.200

a: From Ludwig *et al.*, 1996. F_S stands for the annual sediment flux. F_{POC} is the Particulate Organic Carbon flux (t·km^{-2}·yr^{-1}) at the estuary.

b: From Zhang *et al.*, 1998. E represents the annual erosion intensity.

c: From the Yellow River Conservancy Commission, China.

d: From Li and Liu, 2003.

e: From Smith *et al.*, 2005.

f: From Asselman *et al.*, 2003.

Table 3. Annual mass of sediment transported, soil organic carbon content, *SDR*, *SHC*, *VFR*, and CO_2 flux for Yellow River Basin and the world

Region	T_S ($Gt \cdot yr^{-1}$)	*SDR*	C_{SOC} ($g \cdot kg^{-1}$)	*VFR*	F_T ($Mt \cdot yr^{-1}$)
Yellow River	0.657	0.692	6.15	0.0413	0.235
World	20	0.1	20	0.21	840
Percentage	3.1%		30.8%	19.7%	0.03%

Table 4. Confidence probabilities provided by a Monte Carlo analysis for nine river basins

Basin Name	Frequency of Occurrence			Confidence Probability
	Source	Weak Sink	Strong Sink	
Yellow River	360	536	104	0.536
Yangtze	122	805	73	0.805
Ganges	420	578	2	0.578
Congo	861	139	0	0.861
Niger	146	834	20	0.834
Orange	814	186	0	0.814
Senegal	79	90	831	0.831
Mississippi	246	751	3	0.751
Rhine	87	535	378	0.535

Figure Captions

Figure 1. *SDR–SHC* system for identification of CO_2 source or sink and its strength, on which are plotted results for actual river basins, including the Yellow River Basin.

Figure 2. Soil distribution in the Yellow River Basin.

Figure 3. Time series of sediment yield for the Yellow River at Sanmenxia and Lijin, 1960~2008.

Figure 4. Accumulative erosion-induced CO_2 flux from source to mouth in the Yellow River Basin.

Figure 5. Decade-averaged *VFR* and *SDR* in the Yellow River Basin from 1960 to 2008.

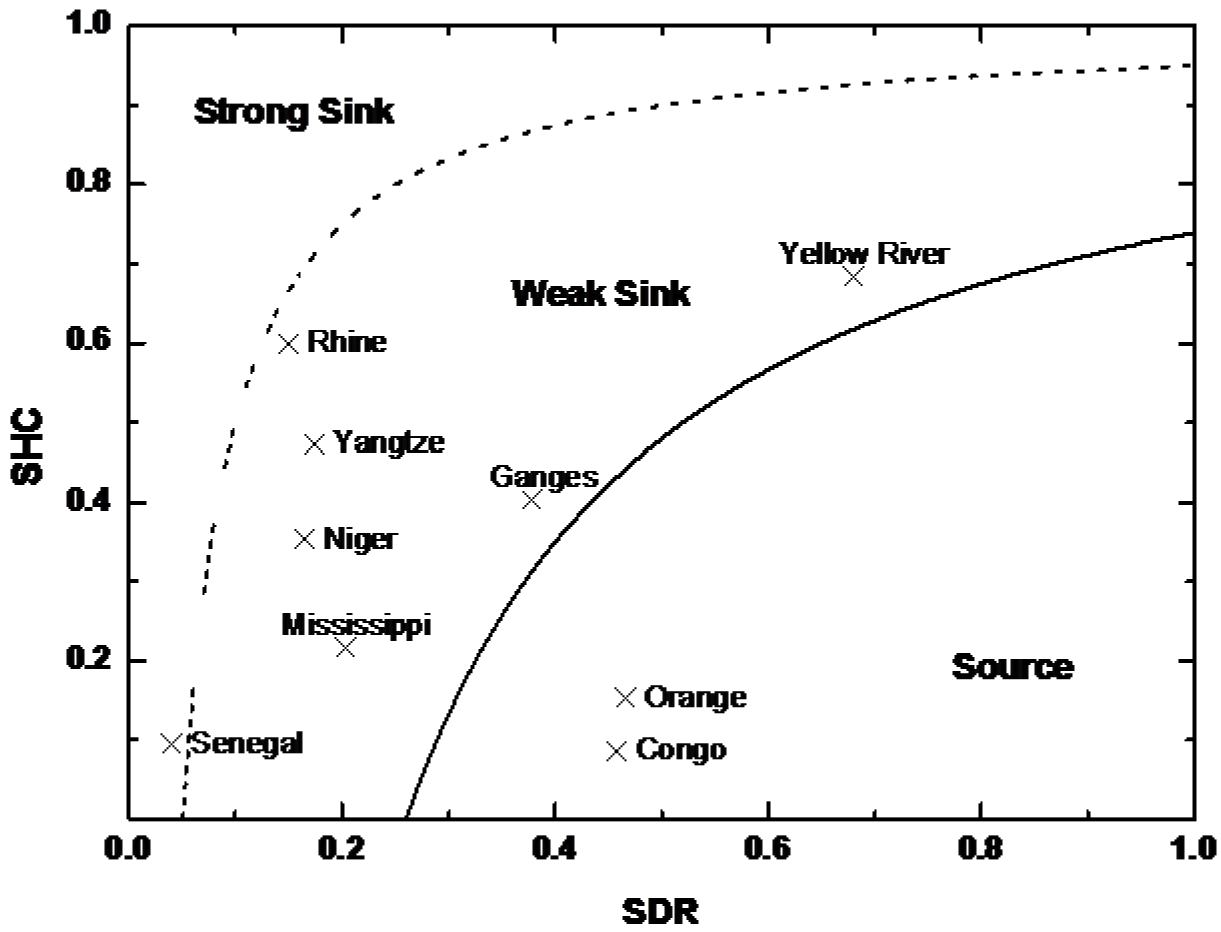

Figure 1. *SDR–SHC* system for identification of CO_2 source or sink and its strength, on which are plotted results for actual river basins, including the Yellow River Basin.

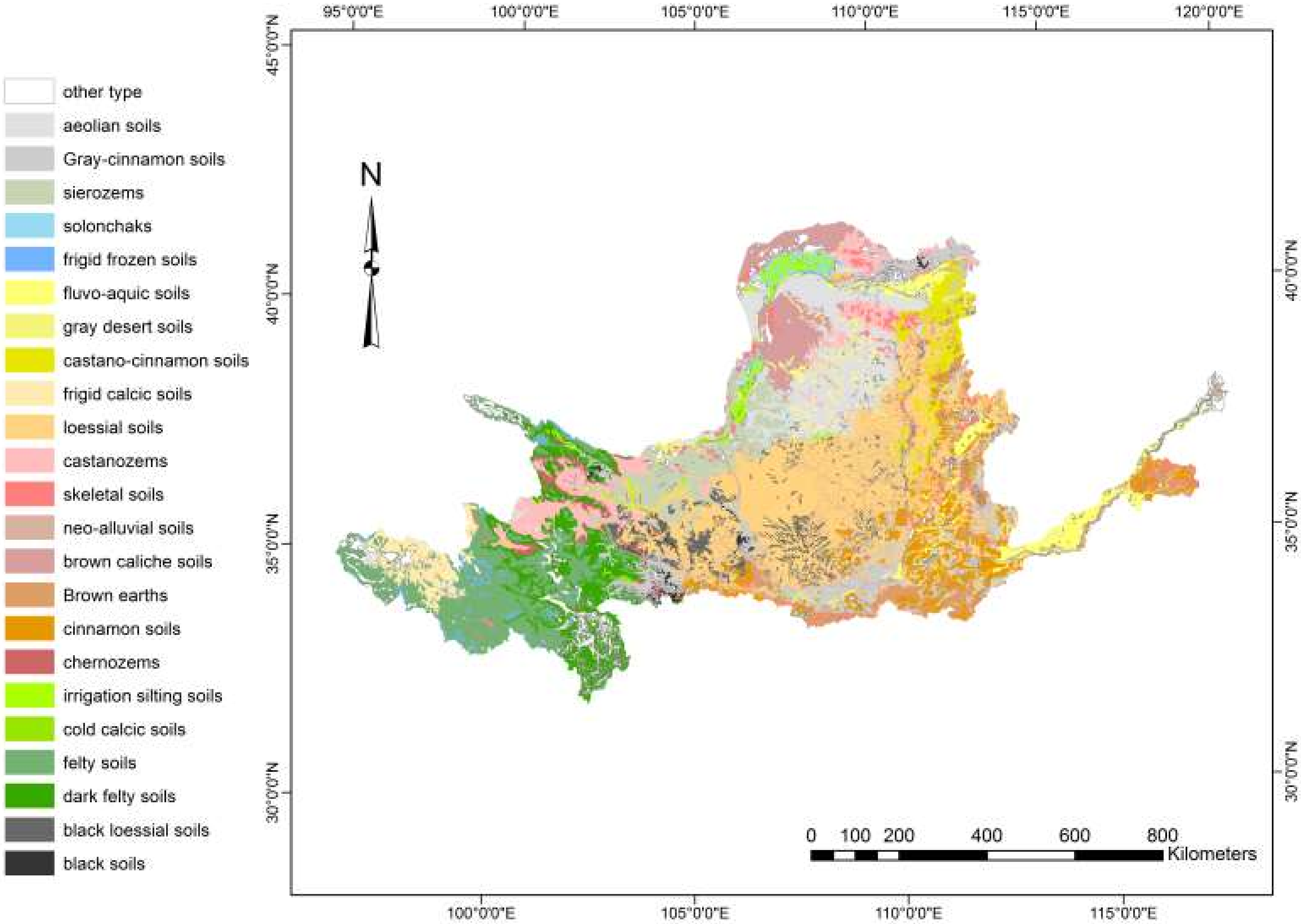

Figure 2. Soil distribution in the Yellow River Basin.

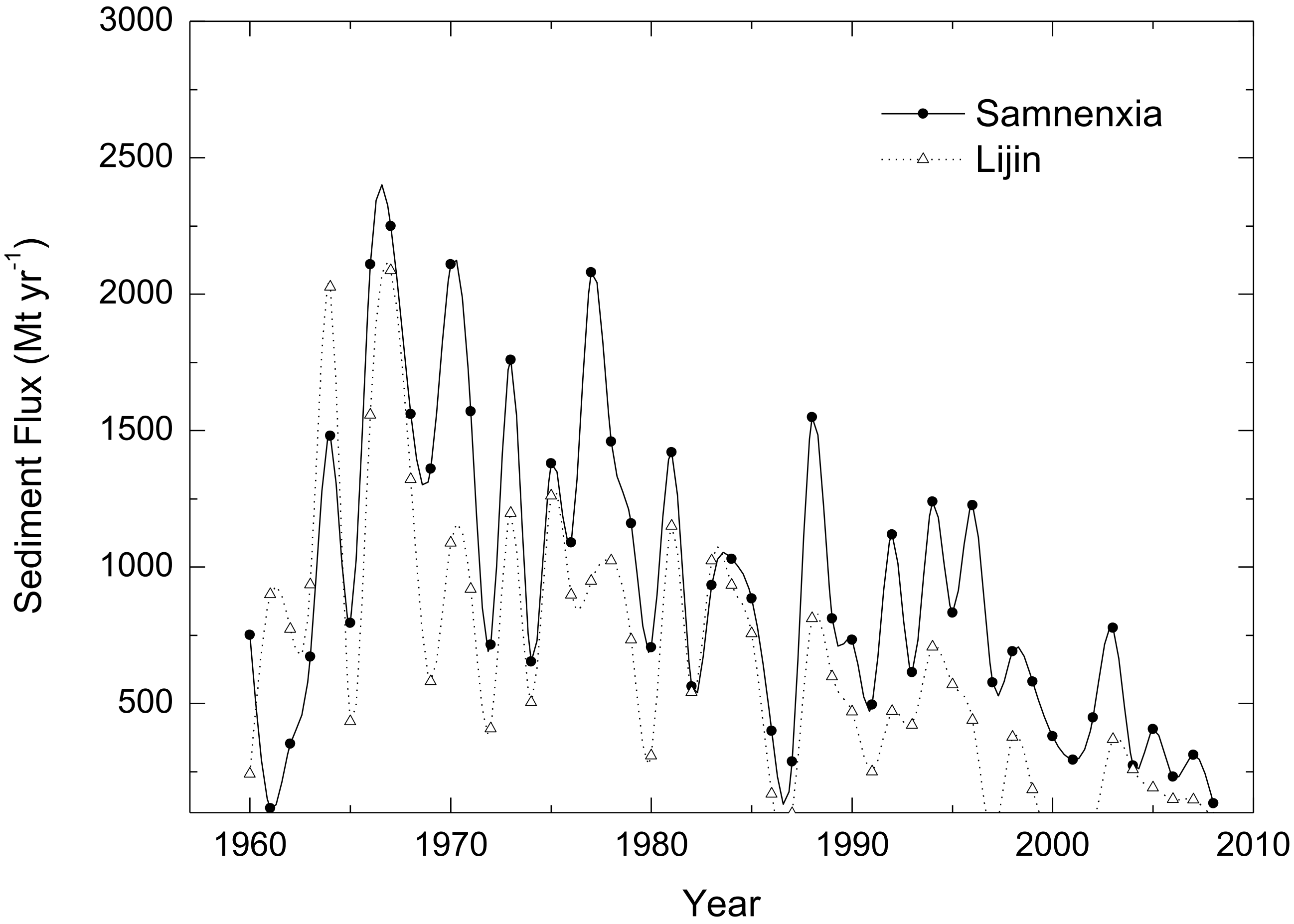

Figure 3. Time series of sediment yield for the Yellow River at Sanmenxia and Lijin, 1960~2008.

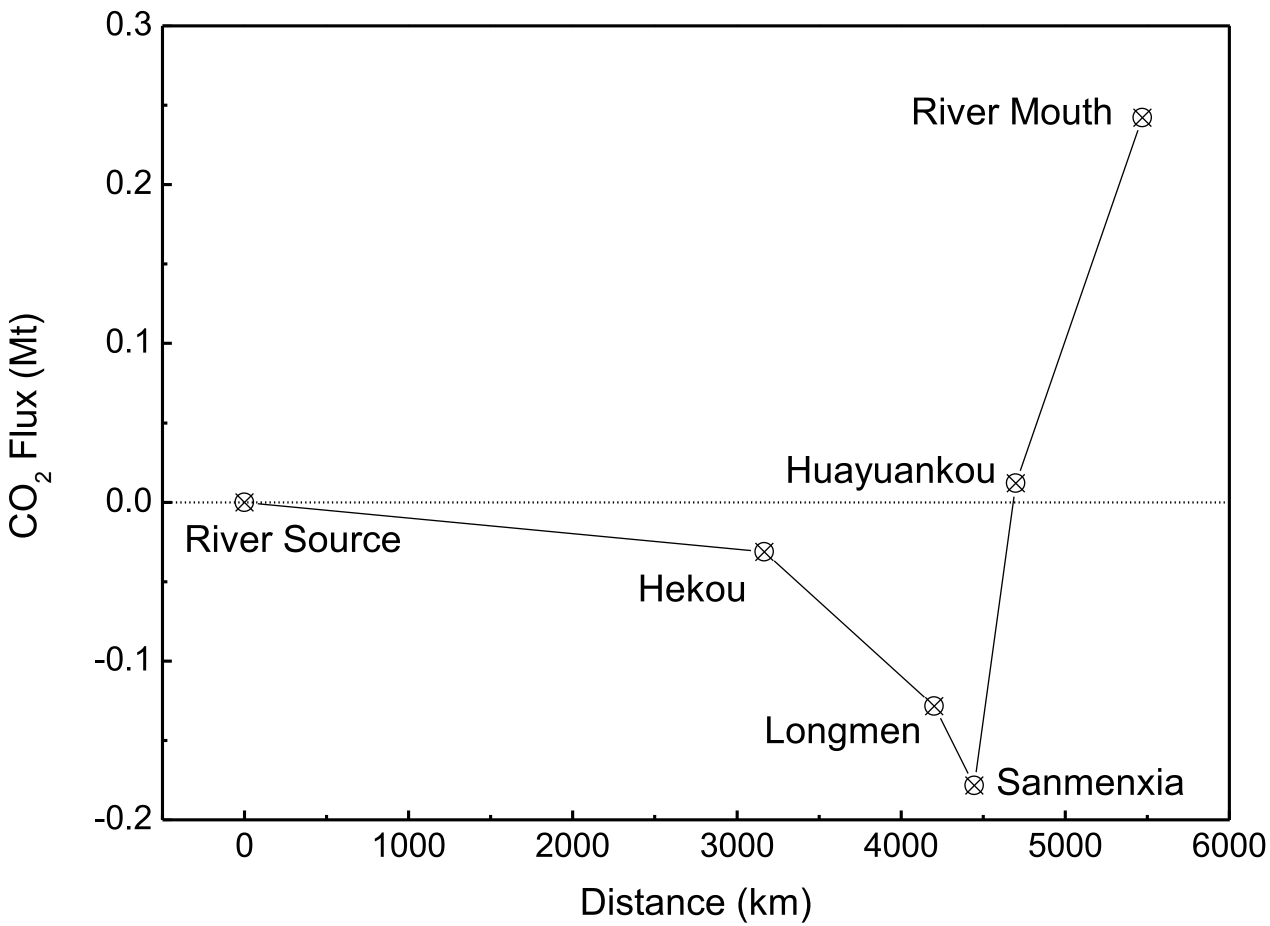

Figure 4. Accumulative erosion-induced CO_2 flux from source to mouth in the Yellow River Basin.

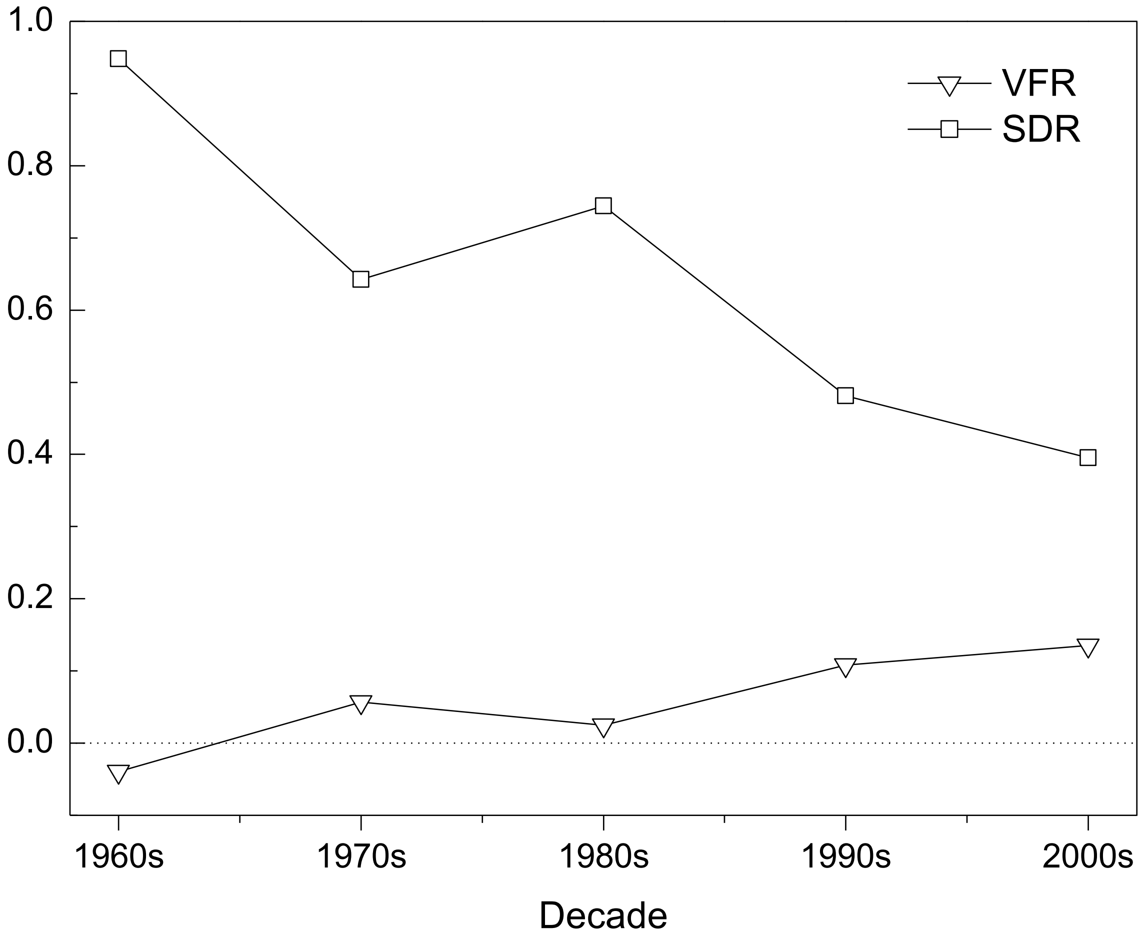

Figure 5. Decade-averaged *VFR* and *SDR* in the Yellow River Basin from 1960 to 2008.